LIMNOLOGY and OCEANOGRAPHY

ASLO

Limnol. Oceanogr. 67, 2022, 450–467

doi: 10.1002/lno.12003

Pond methane dynamics, from microbial communities to ecosystem budget, during summer in Alaska

Carmella Vizza,*,[a] **Stuart E. Jones**, **Julia A. Hart**, **William E. West**, **Gary A. Lamberti**
Department of Biological Sciences, University of Notre Dame, Notre Dame, Indiana

Abstract

Ponds play a larger role in the global freshwater methane (CH_4) budget than predicted from surface area alone. To improve our understanding of pond CH_4 dynamics, we measured summer CH_4 production, concentrations, and emissions to the atmosphere in nine Alaskan wetland ponds along with potential physical, chemical, and biological regulators. Pond CH_4 production (0.64, 0.086–1.3 mmol m^{-2} d^{-1}; median, interquartile range), as assessed with slurry incubations, was positively related to water-column temperature and chlorophyll *a* (Chl *a*), negatively influenced by oxygen levels, and varied with microbial community structure. Average water-column CH_4 concentrations (0.39, 0.21–0.87 μmol L^{-1}) were lower in deeper ponds and at higher oxygen levels, and as expected, they were correlated with diffusive emissions (0.055, 0.024–0.20 mmol m^{-2} d^{-1}) assessed with flux chambers. Based on a mass balance approach, 39–99% of CH_4 produced in ponds was oxidized. Pond ebullition (3.7, 0.60–24 mmol m^{-2} d^{-1}) was higher and more variable than diffusive emissions. Additionally, pond ebullition rates were better correlated with production rates from the previous month. We also systematically compared the ratio of ebullition to diffusive CH_4 emissions in our ponds and other northern lakes, which was negatively related to water depth ($n = 71$), but positively related to Chl *a* ($n = 28$). Our study sheds light on the factors that influence pond CH_4 dynamics and demonstrates that pond ebullition is a significant CH_4 source worthy of continued study.

Recent studies suggest that small ponds may disproportionately contribute to global CH_4 emissions (Holgerson and Raymond 2016; Wik et al. 2016b; Rosentreter et al. 2021). For example, smaller ponds and lakes (< 0.1 km^2) account for around 25% of the global surface area of lakes and ponds, yet the current best estimates suggest that they may produce about three-quarters of CH_4 emissions from those systems (Holgerson and Raymond 2016; Rosentreter et al. 2021). Due to the shallow nature of some smaller lakes and ponds, incorporating CH_4 emissions mediated by plants and those from ebullition (bubbling) is critical to reducing uncertainty in the freshwater CH_4 budget (Rosentreter et al. 2021).

Accurately estimating freshwater CH_4 budgets is challenging and requires a mechanistic understanding of what regulates the sources and sinks of CH_4. Previous research suggests that organic matter supply and microbial community structure influence CH_4 production in both ponds and lakes (Vizza et al. 2017a; Bertolet et al. 2019; Grasset et al. 2021). Specifically, primary production increases the amount of carbon available in the sediments (Juutinen et al. 2003; Rasilo et al. 2015), but the source of that carbon is also important for methanogens, or the microbial organisms responsible for CH_4 production. For example, West et al. (2012) found that algal additions had a greater effect on CH_4 production in lake sediments than maple leaves thus corroborating the well-established principle that autochthonous or aquatic sources are more readily preferred by microbes than allochthonous or external carbon sources (Kritzberg et al. 2004). However, not all autochthonous sources of carbon are created equal, which has been demonstrated by (1) Vizza et al. (2017a) who found that only a subset of aquatic plant additions enhanced CH_4 production in pond sediments; (2) Grasset et al. (2018) who found that while one aquatic plant enhanced CH_4 production as much as phytoplankton, another species matched the lower rates from an allochthonous source; and (3) Grasset et al. (2019) who observed that macrophytes with high water

*Correspondence: carmella.vizza@gmail.com

Additional Supporting Information may be found in the online version of this article.

[a]Present address: College of Natural and Computational Sciences, Hawai'i Pacific University, Kaneohe, Hawaii, USA

Author Contribution Statement: C.V., S.E.J., and G.A.L. designed the study. C.V. and J.A.H. performed the research. W.E.W. analyzed CH_4 samples. C.V. wrote the paper with contributions from all co-authors.

content and lower C/N ratios induced higher CH_4 production rates. Therefore, both organic matter quality and quantity (Grasset et al. 2021), as well as the microbial communities utilizing the organic matter, can influence CH_4 production in aquatic ecosystems.

To better quantify the sinks and sources of CH_4, we must consider the factors that govern the processes of CH_4 oxidation and emissions. The process of CH_4 oxidation can be limited by the availability of CH_4 and O_2 (Segers 1998), but O_2 can also be inhibitory at high concentrations (Thottathil et al. 2019). Additionally, deeper water layers tend to have greater oxidation rates because stratification can lead to more CH_4 buildup and thus increases the likelihood that CH_4 is oxidized at the sediment–water interface or even in the water column (Bastviken et al. 2002a, 2008). Additionally, CH_4 can build up in stratified aquatic ecosystems for months at a time before being released during seasonal turnover (Riera et al. 1999). While diffusive emissions are often affected by wind speed, turbulence, and surface area (Vachon et al. 2019; Deemer and Holgerson 2021; MacIntyre et al. 2021), West et al. (2016) showed that shallow water depths and greater CH_4 productions rates could be predictive of higher lake ebullition. Additionally, Deemer and Holgerson (2021) found that ebullition in 116 lakes was positively associated with chlorophyll *a* (Chl *a*). Therefore, understanding how CH_4 oxidation and emissions are affected by these physical, chemical, and biological factors will be key in predicting pond CH_4 budgets.

Understanding how CH_4 dynamics are affected by biological, physical, and chemical factors is important for estimating the impact of freshwater systems on the global CH_4 budget. In this study, we surveyed pond CH_4 production, water-column concentrations, diffusive emissions, and ebullition in nine Alaskan ponds varying in size (0.004–0.2 km^2). Our primary objectives were (1) to identify biological, physical, and chemical factors that influenced pond CH_4 dynamics during the summer; 2) to determine whether the summer CH_4 dynamics in these ponds could be balanced with a budget approach; and (3) to compare the relative importance of ebullition to diffusive emissions in these Alaskan ponds and previously studied northern lakes. We hypothesized that pond CH_4 production would be regulated by substrate supply and microbial communities, while CH_4 emissions would be regulated by physical and chemical factors. Additionally, we hypothesized that the ratio of ebullition to diffusive emissions would be higher in these Alaskan ponds relative to other systems due to their shallow depths and high productivity.

Methods

Study area

The Copper River Delta in southcentral Alaska is the largest contiguous wetland along the Pacific Coast of North America with about 283,000 ha of habitat supporting high biodiversity (Bryant 1991). The Great Alaska Earthquake of 1964 elevated the Copper River Delta by 1–4 m depending on location, thereby uplifting and creating numerous wetland ponds (Thilenius 1995). Ponds are distributed across the continuum of glacial headwaters to the Gulf of Alaska with variable physical and chemical characteristics and ecosystem processes (Vizza et al. 2017b). Many of these ponds are predominantly precipitation-fed since many became hydrologically isolated during the 1964 earthquake. These ponds are embedded within a wetland landscape where the discrete transition from wetland to pond is often marked by the end of a *Sphagnum* spp. mat, followed by a fringe of *Menyanthes trifoliata* or *Carex* spp., and finally substantially deeper water (> 0.3 m). Vegetation covers < 25–75% of a pond's water surface with the dominant emergent macrophytes consisting of *Nuphar polysepalum*, *Hippuris vulgaris*, and *Equisetum variegatum* (Table S1). Submerged vegetation (*Fontinalis* spp. and *Myriophyllum* spp.), when present, often covers more than 67% of the benthos (Table S1). Our study focused on nine ponds (Table 1) that we were able to access regularly. During the summer of 2014, the study ponds were visited on three occasions (late June, mid-July, and early August) either in the morning or early afternoon at approximately 3-week intervals. We measured CH_4 dynamics along with potential physical, chemical, and biological regulators (Fig. S1) during each sampling occasion.

Physical and chemical parameters

We measured water depth, dissolved oxygen (DO), and temperature for each pond, while wind speed data were obtained from the nearby airport. Water depth was measured at each site where sediment was collected using a stadia rod ($n = 5$ per pond per sampling period). We also measured DO in the lower water column (i.e., ~ 0.4–0.8 m below the surface depending on the pond's depth) at each sampling period using an YSI Pro Plus multiparameter water quality meter (YSI). Additionally, water-column temperature was measured hourly using a HOBO Pendant Temperature Logger (Onset Computer Corporation), which was deployed in the center of each pond at a water depth of 0.1 m. Temperature, as measured with a YSI, did not vary with depth during most sampling events, while DO was more variable (Table S2). The daily average wind speed was determined from hourly recordings at the Merle K. (Mudhole) Smith Airport located centrally on the west side of the Copper River Delta (4–26 km away from each pond). These quality-controlled climatological data were provided by National Centers for Environmental Information (National Oceanic and Atmospheric Administration) with each station using an anemometer to measure wind speed at a height of approximately 10 m.

Substrate quantity and quality

These Alaskan ponds often had floating algae associated with submerged macrophytes and sometimes emergent vegetation. Chl *a* in the water column was positively correlated with vegetation cover ($r_P = 0.90$, $n = 9$, $p < 0.001$); vegetation cover was scored on a scale of 1–7 after ranking ponds on a scale of 1–3 for submerged vegetation in increasing

Table 1. Location and size of the nine wetland ponds in the Copper River Delta, Alaska.

Pond	Latitude (°N)	Longitude (°W)	Elevation (m)	Surface area (m^2)
Eyak N (EYN)	60.492	−145.661	5.2	6670
Eyak S (EYS)	60.477	−145.683	5.5	6640
Lily (LIL)	60.520	−145.601	8.2	20,540
Rich Hate Me (RHM)	60.478	−145.382	18.3	3570
Scott S (SCS)	60.491	−145.547	13.4	10,370
Storey N (STN)	60.323	−145.161	4.6	151,750
Storey S (STS)	60.306	−145.178	2.1	177,490
Tiedeman N (TIN)	60.431	−145.466	5.5	6770
Tiedeman S (TIS)	60.425	−145.473	5.5	57,000

increments of 33% and 1–4 for emergent vegetation in increasing increments of 25% and combining the submerged and emergent scores (Table S1). Due to this positive correlation and the existence of temporal measurements, we used Chl *a* instead of vegetation cover as an index of productivity (Wetzel and Likens 2000).

We collected 1 liter of water from the water column at three different sites per pond per sampling period. Water samples (100–200 mL) were filtered through glass fiber filters (Whatman GF/F, 0.7-μm pore size), and these filters were frozen until analysis. Filters were processed and analyzed for Chl *a* after Steinman et al. (2017). We extracted the filters in 10 mL of 90% buffered acetone overnight and used a fluorometer (TD-700; Turner Designs), which was calibrated with Chl *a* analytical standards, to analyze the sample for Chl *a* the following day.

We collected sediment samples (~ 250 mL, up to a 20-cm depth) from five sites per pond per sampling event using a handheld bucket augur. Two subsamples of the sediment were frozen for later analysis of (1) sediment organic matter (SOM) and (2) microbial community structure, while the remaining sediment was used to estimate methane production (see the Methane production estimates section for more information). The sediment was dried for at least 48 h at 60°C, the dry weight was recorded, and then the organic matter in the sediment was combusted at 500°C in a muffle furnace for 4 h. Finally, the sediment was rewetted with deionized water and then dried at 60°C for at least 48 h before reweighing. SOM was estimated as the percent of material lost during combustion. To extract pore water from the sediment, ~ 50 mL of the sediment was centrifuged for 45 min at 4°C at 4000 RCF (relative centrifugal force). This pore water was then analyzed on the Dionex ICS-5000 (Dionex Corporation) for acetate and sulfate; for more details please see Vizza et al. (2017a).

Microbial community structure

To characterize the microbial community structure of each pond, DNA was extracted from a composite of the five sediment samples from each of the nine ponds for the June time period ($n = 9$) as described in Vizza et al. (2017a). Two genes, methyl coenzyme reductase (*mcr*) and dissimilatory sulfite reductase (*dsr*), were targeted with quantitative PCR (qPCR). The *mcr* gene catalyzes the final step of reducing a methyl group to CH_4 (Thauer 1998), and its ubiquity in methanogens makes it powerful at assessing their abundance (Luton et al. 2002; Earl et al. 2003; Castro et al. 2004). The *dsr* gene catalyzes the last step in sulfate respiration and is possessed by all sulfate-reducing bacteria, making it ideal to quantify their abundance (Wagner et al. 1998; Klein et al. 2001; Zverlov et al. 2005). Specifically, we used the ratio of *mcr* : *dsr* as a means of characterizing microbial community structure at each pond. This characterization was appropriate across the entire 6 weeks of sampling because previously microbial community structure did not change over the course of a few weeks even when exposed to different conditions (i.e., flooding pond sediments with sulfate-rich, brackish water per Vizza et al. (2017a)). More details about amplification and qPCR can be found in Vizza et al. (2017a).

Methane production estimates

Because sediment samples (up to 20 cm in depth) were collected from five sites that were representative of the pond's habitat (i.e., each site corresponded to ~ 20% of the pond area), CH_4 production rates inferred from the incubation of sediment from each site were averaged to generate a whole-pond estimate. Methane production rates were estimated from 2-week anaerobic sediment slurry incubations after Vizza et al. (2017a). For each incubation, approximately 50 mL of sediment and 60 mL of unfiltered pond water were incubated in a 250-mL serum bottle in the dark. Each bottle was made anoxic by vigorously swirling and purging it with N_2 gas for 5 min. Headspace samples (10 mL) were removed at five intervals (2, 5, 8, 11, and 14 d) and injected into individual 2-mL serum vials (pre-evacuated with a vacuum pump), and stored upside down in water for less than 3 months until the samples could be analyzed using gas chromatography. To maintain pressure in the incubations, 10 mL of N_2 gas was added after each sampling point, which was accounted for in the calculations. All headspace samples were analyzed after West et al. (2016) on an Agilent 6890 Gas Chromatograph. Because all headspace samples had positive pressure when analyzed, we were not concerned about sample dilution during storage.

Since the incubation temperature (14–15°C) was slightly lower than the average pond temperature (June: 17.3°C ± 0.9°C, July: 17.2°C ± 1.2°C, August: 18.4°C ± 1.2°C), CH_4 production estimates were considered conservative. Production rates were inferred from the slope of the linear regression of CH_4 concentrations over time per incubation, which were converted to areal rates by assuming an active sediment depth of 20 cm such that the average incubation (~ 50 mL of sediment) represents about 0.01 m^2 of pond sediment surface area. We chose this active sediment depth based on other studies (Kelly and Chynoweth 1981; Schwarz et al. 2008; West et al. 2016) and because we believed it be conservative considering observations of CH_4 production as deep as 60–70 cm (Banning et al. 2005). Over the course of the study, we conducted a total of 135 incubations (9 ponds × 3 sampling events × 5 sites). The production rates of 10 incubations out of 135 were excluded from analyses because their r^2 values from linear regressions of CH_4 over time were lower than 0.5; the remaining 125 rate estimates had r^2 values of 0.86 ± 0.12 (mean ± SD).

Water-column CH_4 concentrations

To measure CH_4 concentrations in the water column, water samples were collected at three different sites per pond per sampling event at a surface depth (0.1 m) and a bottom depth just above the sediment (0.3–0.8 m) for a total of 162 samples (9 ponds × 3 sampling events × 3 sites × 2 depths). Generally, water depth did not vary across the three sites within a pond (< 10%) at any single sampling event. We used a Van Dorn (horizontal water) sampler with an airtight valve installed on the side to collect the water and then transferred it to a 60-mL syringe equipped with a gastight valve. Upon returning to the lab, 15 mL of N_2 was added to 45 mL of water for each sample, shaken vigorously, and allowed to equilibrate for 30 min. All headspace samples were stored and analyzed like the production samples. We then converted the analyzed headspace concentrations to water-column CH_4 concentrations using Henry's Law (Griffiths et al. 1982). Methane concentrations for each sampling event did not vary by depth within a pond (repeated measures ANOVA: $p > 0.80$) and are therefore presented and analyzed as cross-depth means. We excluded seven samples where the benthos was unintentionally disturbed, which increased the coefficient of variation (CV) above 1 for a pond's sampling event, as well as two statistical outliers that were three standard deviations higher than the mean.

Methane emissions

Methane emissions to the atmosphere were estimated after West et al. (2016) using five floating chambers (0.062 m^2, 6.3 L) placed in open water per pond per sampling event. We avoided including emergent vegetation in the chambers, and therefore did not quantify plant-mediated CH_4 emissions during this study. At the end of each 1.5-h deployment, we mixed the chamber headspace with a 10-mL syringe at least three times and then withdrew 10 mL of gas for a total of 135 samples (9 ponds × 3 sampling events × 5 chambers). To determine the atmospheric concentration of CH_4, three 10-mL air samples were collected above each pond for each sampling event for a total of 81 samples (9 ponds × 3 sampling events × 3 replicates). The average atmospheric CH_4 concentration across all ponds and sampling events was 5.2 ± 1.6 ppm. All flux chamber and atmospheric samples were stored and analyzed in the same manner as the production and concentration samples.

To estimate chamber-based emission rates, we first calculated the rate of change in CH_4 concentration, which is the chamber CH_4 concentration minus that of the atmosphere based on deployment length (~ 1.5 h or 0.0625 d), multiplied by the chamber's volume and divided by its surface area. Because the diffusive flux of gas into a chamber decreases over time in a nonlinear fashion as it becomes more concentrated, we also calculated instantaneous emission rates to correct for this nonlinear response as detailed in Bastviken et al. (2004). However, this method cannot calculate rates when the concentration of CH_4 in the chamber is much higher than expected if it were in equilibrium with the surface water CH_4 concentration; this happened in 20 out of 135 cases. Due to short deployment periods, chamber-based rates were roughly equivalent to instantaneous rates with only an average 6% difference. Therefore, we chose to report and analyze chamber-based rates since these rates could be calculated for an additional 20 chambers; 10 chambers with negative emissions to the atmosphere were excluded from analyses after comparison to other chambers from that sampling event deemed a leak likely.

To determine whether CH_4 emissions were impacted by diffusion or ebullition, we used the method first proposed by Bastviken et al. (2004) and later by Cole et al. (2010), which was verified to accurately estimate ebullition 86% of the time by Barbosa et al. (2021). Briefly, we calculated a chamber-based k_{600} by calculating a chamber-based k_{CH_4} as described in Cole et al. (2010):

$$k_{CH_4} = \frac{V}{K_h RTA} \ln\left(\frac{P_w - P_i}{P_w - P_f}\right) / (t_f - t_i) \quad (1)$$

where V is the chamber volume in (m^3), K_h is the Henry's law constant for CH_4 (moles m^{-3} Pa^{-1}), R is the gas constant (8.314 m^3 Pa K^{-1} mol^{-1}), T is the temperature (K), A is the area of the chamber (m^2), P_w is the partial pressure (Pa) of CH_4 in the water, P_i is the initial partial pressure (Pa) of CH_4 in the chamber, and P_f is the final partial pressure (Pa) of CH_4 in the chamber.

Then, we normalized k_{CH_4} to a Schmidt number of 600 as described in Cole et al. (2010):

$$k_{600} = \left(\frac{600}{Sc_{CH_4}}\right)^n k_{CH_4} \quad (2)$$

where $n = -0.5$, a value appropriate for low-wind systems, and Sc_{CH_4} is the Schmidt number as calculated from Matthews et al. (2003):

$$Sc_{CH_4} = 1897.9 - 114.28t + 3.2902t^2 - 0.039061t^3 \quad (3)$$

where t is the temperature in °C.

If the chamber-based k_{600} was more than double the k_{600} of the minimum chamber for a given pond on a given sampling date, that chamber was considered impacted by ebullition. We also considered the 20 flux chambers where we could not calculate instantaneous rates or k_{600} impacted by ebullition. Additionally, we believe that all five chambers at Tiedeman North in July and all five chambers at Tiedeman South in August were impacted by ebullition because their minimum k_{600} values were more than an order of magnitude higher than the median value for all pond/sampling event combinations (i.e., 2.4 and 2.7 in comparison to 0.24). The k_{600} values for all 10 chambers (i.e., 5 at Tiedeman North in July and 5 at Tiedeman South in August) were also at least four times greater than their k_{600} values based on wind speed (Cole and Caraco 1998); therefore, these 10 chambers were classified as ebullition. We captured ebullition in approximately 63% of our flux chambers. Diffusive CH_4 emission rates and ebullition rates were then averaged on an arithmetic basis as the five flux chambers were placed in areas representative of each pond.

Dissolved CH_4 budgets, oxidation estimates, and water-column $\delta^{13}CH_4$

We created dissolved CH_4 budgets for the two 3-week intervals that elapsed during our sampling events. First, we averaged CH_4 production and diffusive emission rates for the interval's start and end sampling date. These areal rates were then converted to changes in volumetric concentrations (mmol m^{-3}) by multiplying by the interval length and the surface area of the pond and then dividing by the pond volume, which is pond surface area multiplied by mean depth. We also calculated the change in CH_4 concentration in water-column samples from the start and end sampling date, which should reflect the balance of CH_4 inputs and outputs. Possible inputs are pond CH_4 production and any external CH_4 inputs including hydrologic sources, while possible outputs are CH_4 oxidation in the water column, diffusive CH_4 emissions, and other outputs (e.g., hydrologic outflow). We assumed that hydrologic CH_4 inputs and outputs were negligible because the primary hydrologic source of a subset of our study ponds across the glacial headwater to ocean continuum was confirmed to be precipitation using piezometers (Luca Adelfio, U.S.D.A. Forest Service, unpubl. data). Therefore, our simplified mass balance equation was:

$$\Delta\text{water} - \text{column}\,CH_4 = \text{production} - \text{oxidation} - \text{diffusive emissions} \quad (4)$$

We then solved for oxidation and calculated the percentage of CH_4 produced that was oxidized (Table S3).

For these simplified budget calculations, we assumed that the CH_4 produced in our incubations had only three potential fates—temporary storage in the water column as dissolved CH_4, oxidation, or diffusive flux to the atmosphere—and that budgets could be balanced with oxidation over the 3-week interval. We ignored ebullition in the budget calculations for two reasons: (1) laboratory production assays are unlikely to mimic pond bubbling after the destruction of sediment macropores and (2) ebullition is a quick process likely to bypass dissolution or oxidation in the water column (Walter et al. 2008), especially in shallow systems. If laboratory production assays indeed capture pond bubbling activity that would normally bypass oxidation, then we may be overestimating how much CH_4 moves from the sediments into the water column and therefore how much is oxidized. In contrast, any external inputs not accounted for would increase the water-column CH_4 concentration, thus leading to an underestimate of oxidation.

Because we acknowledge that our measurements were more spatially than temporally robust for such a budget approach, we tested the assumptions made in our dissolved CH_4 mass balance calculations by measuring stable carbon isotope signatures ($\delta^{13}C$) of CH_4 on two occasions in each pond. Methane oxidation discriminates against the heavier ^{13}C isotope (Whiticar 1999), so we can expect CH_4 in the water column to be enriched in ^{13}C relative to the source, which should be proportional to the magnitude of CH_4 oxidation occurring there (Bastviken et al. 2002b). Generally, acetotrophic and methylotrophic methanogenesis produce CH_4 with a $\delta^{13}C$ of −70‰ to −50‰, while hydrogenotrophic methanogenesis can range from −120‰ to −60‰ (Whiticar 1999). Because our previous research has demonstrated that acetate is important for methanogens in these ponds (Vizza et al. 2017a), we assumed that the $\delta^{13}C$ of CH_4 produced in the sediments would exhibit a relatively narrow range as long as the source was not hydrogenotrophic methanogenesis. Any variation in $\delta^{13}C$ of CH_4 sources or in the methanogen and methanotroph communities would only decrease our ability to detect a relationship with oxidation estimates as would any external CH_4 inputs or outputs that were unaccounted for, therefore resulting in an even stricter test of our assumptions. Nevertheless, it is important to note that detecting a correlation between $\delta^{13}CH_4$ and our mass-balance-based oxidation rates provides support for relative, but not absolute, differences in oxidation rates between these ponds.

To measure $\delta^{13}C$ of CH_4 in the water column, we collected water samples directly above the sediment and any submerged vegetation using a Van Dorn sampler during July and August (9 ponds × 2 sampling events × 2 sites). Methane was collected and extracted from the water column as detailed in West et al. (2016) and the Water-column CH_4 concentrations section, but these samples were stored in 12-mL exetainers flipped upside down in tap water. They were analyzed within 6 months on a Thermo Delta V Advantage interfaced with a Thermo Gasbench II/Precon at the University of Notre Dame Center for Environmental Science; instrumental precision

was < 0.2 ‰. Isotopic data are reported in δ notation (‰) relative to the Pee Dee belemnite standard where $\delta^{13}C = ([R_{sample} - R_{standard}] - 1)$, and R is the $^{13}C/^{12}C$ ratio. We were unable to detect a large enough CH_4 peak to obtain $\delta^{13}C$ values for 17 of the 36 samples.

Statistical analyses

To determine which factors influenced CH_4 production, concentrations, diffusive emissions, and ebullition, we used mixed-effect model selection after Zuur et al. (2009), which includes checking for collinearity among predictor variables. The candidate predictor variables that we included in the full model for each response variable are detailed in Fig. S1 and Table S4. Any predictors that were characterized at the pond-level only once such as pond surface area and microbial community structure (i.e., the ratio of methanogens relative to sulfate-reducers or *mcr* : *dsr*) had the same values for each sampling event. Pond was included as a random factor for each model to account for pseudoreplication incurred from repeated sampling at the site level, and variables with right-skewed distributions were $\log_{10}$-transformed to better meet assumptions of normality. We calculated a pseudo-r^2 for each best-fit model to partition variance between the fixed effects and random effects after Nakagawa et al. (2017). Additionally, we conducted a linear regression of the observed data vs. data predicted from the model parameters for all four of the response variables. For each regression line, we conducted two-tailed *t*-tests to determine whether the slope differed from 1 or the intercept differed from 0 (Zar 2010). To test the assumptions of our mass-balance-based oxidation rates, we created a mixed-effect model with the percentage of CH_4 oxidized as the response variable, pond as a random factor, and water-column $\delta^{13}CH_4$ as a fixed factor. Because ebullition rates often exceeded production estimates, we thought it possible that ebullition might be integrating CH_4 production over larger spatial and temporal scales, especially since the physics of bubbling are characterized by a critical threshold that must be overcome (Peltola et al. 2018). To examine the possibility of temporal integration, we investigated whether ebullition rates were influenced by the previous month's production rates. We therefore created a single mixed-effect model with ebullition rates from both July and August as the response variable, pond as a random factor, and the previous month's production rates (i.e., June for July ebullition and July for August ebullition) as the fixed factor. We conducted all statistical analyses in R, using a significance level of $\alpha = 0.05$ for parametric tests.

We also conducted a systematic comparison of the ratio of ebullition to diffusive CH_4 emissions by combining our data from nine ponds with the 40 Alaskan lakes in Sepulveda-Jauregui et al. (2015), the 3 Canadian lakes in DelSontro et al. (2016), the 16 Wisconsin lakes in West et al. (2016), and the 3 Swedish lakes in Jansen et al. (2019). We calculated the ratio from the average summer emissions of each site for ebullition and diffusion ($n = 71$). Then, we analyzed how the ratio of ebullition to diffusive CH_4 emissions was influenced by both maximum depth and area; all variables were $\log_{10}$-transformed, and study was included as a random factor. For the three Canadian lakes, we used mean depth because maximum depth was not reported (DelSontro et al. 2016). Finally, using the subset of studies with water chemistry data (DelSontro et al. 2016; West et al. 2016) including our own ($n = 28$), we used mixed-effect model selection to determine what physical (i.e., mean depth and area) and chemical variables (i.e., total phosphorus, Chl *a*, and dissolved organic carbon) influenced the ratio of ebullition to diffusive CH_4 emissions with study as a random factor. Because we did not measure total phosphorus data for these ponds in 2014, we used 2013 data instead. Again, variables with right-skewed distributions were $\log_{10}$-transformed to better meet assumptions of normality.

Results

Methane production

Methane production rates were variable across the summer (Table 2; Fig. 1a) and related to biological, physical, and chemical factors. The best-fit model therefore included pond as a random effect and DO in the lower water column just above the benthos (DO; $p = 0.004$), water-column Chl *a* ($p = 0.02$), the ratio of methanogens to sulfate-reducers (*mcr* : *dsr*; $p = 0.07$), and water temperature ($p = 0.07$), as fixed effects (Table 3); pond and fixed effects explained 2% and 49% of the variation in CH_4 production rates, respectively. In addition, the observed vs. predicted values from the best-fit model did not statistically differ from the 1 : 1 line (H_0: slope = 1 and intercept = 0, $p \geq 0.9$ for both *t*-tests, df = 25; Fig. 1b). While some microbial and substrate supply predictors were positively related to CH_4 production as hypothesized (Table 3; Fig. S1), the inclusion of SOM or pore-water acetate and sulfate availability did not significantly enhance fit, but sulfate did have a negative effect in one of the top four models with a $\Delta AIC_c < 1$ (Table S4).

Methane concentrations

Water-column CH_4 concentrations varied across ponds and by water depth, but not consistently by sampling month (Table 2; Fig. 1c). The best-fit model therefore included pond as a random effect and depth ($p = 0.02$) as a fixed effect (Table 3). The spatial heterogeneity captured by the random effect explained 61% of the variation in CH_4 concentrations, while pond depth had a negative effect as hypothesized (Table 3; Fig. S1), explaining 18% of the variation. This model accurately predicted observed CH_4 concentrations with the best-fit line of observed vs. predicted values corresponding closely to the 1 : 1 line (i.e., H_0: slope = 1 and intercept = 0, $p \geq 0.35$ for both *t*-tests, df = 23; Fig. 1d). Neither CH_4 production rates nor physical and chemical factors other than water depth (i.e., pond surface area,

Table 2. Pond physical and chemical characteristics and estimates of CH_4 production, water-column CH_4 concentrations, diffusive emissions, and ebullition (mean ± SD; for ebullition only: mean [CV]) in nine Alaskan ponds in summer 2014. The wind speed and water-column temperatures (Temp) listed are the daily averages for the date sampled. Mean DO measured in the lower water column, water-column Chl *a*, SOM, water depth, pore-water acetate, and sulfate levels are also reported. The ratio of *mcr* to *dsr* is an indicator of microbial community structure in the sediments, specifically the abundance of methanogens relative to one of their competitors, sulfate-reducers; this ratio was only measured during the June sampling event. In some sampling events, diffusive emissions or ebullition were not detected (ND); diffusive or ebullition measurements were included in the average only if detected in the flux chambers.

Pond	Date sampled	Depth (m)	Wind speed ($m\ s^{-1}$)	Temp (°C)	DO ($mg\ L^{-1}$)	Chl *a* ($\mu g\ L^{-1}$)	SOM (%)	Acetate ($nmol\ g^{-1}$)	Sulfate ($nmol\ g^{-1}$)	*mcr* : *dsr*	CH_4 production ($mmol\ m^{-2}\ d^{-1}$)	CH_4 concentration ($\mu mol\ L^{-1}$)	Diffusive CH_4 emissions ($mmol\ m^{-2}\ d^{-1}$)	CH_4 ebullition ($mmol\ m^{-2}\ d^{-1}$)
EYN	25 Jun 2014	0.60	1.7±1.2	15.1	9.4	9	1.8	53	202	4.1	0.14±0.04	0.37±0.18	0.01	0.14[0.3]
	16 Jul 2014	0.59	1.2±1.1	17.5	5.6	31	1.8	210	93		1.53±1.48	0.33±0.07	0.004	0.57[1.2]
	04 Aug 2014	0.66	4.0±2.9	18.0	5.7	53	2.2	61	97		1.37±0.80	42.9±18.5	0.91±0.15	600[1.1]
EYS	25 Jun 2014	0.66	1.7±1.2	16.1	7.7	13	1.7	16	90	1.8	0.04±0.05	0.12±0.01	0.02	12[1.7]
	16 Jul 2014	0.66	1.2±1.1	18.6	6.5	11	2.9	30	53		0.67±0.40	0.12±0.03	0.04±0.01	23[1.7]
	04 Aug 2014	0.70	4.0±2.9	18.8	4.3	20	1.9	21	33		0.19±0.15	0.28±0.06	0.08	0.86[0.6]
LIL	23 Jun 2014	0.64	1.7±1.8	14.2	2.4	3	2.5	73	5	20	0.17±0.10	0.85±0.63	0.01	41[2.0]
	14 Jul 2014	0.65	2.3±2.5	16.7	4.3	6	1.3	3	5		2.86±1.32	0.51±0.3	0.09±0.03	0.56[1.0]
	05 Aug 2014	0.66	2.8±1.2	15.1	1.6	13	1.8	44	6		1.47±0.66	35.6±16.0	0.51±0.16	0.89[0.1]
RHM	23 Jun 2014	0.42	1.7±1.8	12.6	2.8	1	3.3	45	20	4.1	0.01±0.01	2.66±1.54	0.20±0.02	ND
	14 Jul 2014	0.38	2.3±2.5	14.9	2.5	4	1.5	17	7		1.44±2.79	3.66±1.98	0.25±0.08	1.1[0.3]
	05 Aug 2014	0.65	2.8±1.2	14.1	0.2	1	5.1	30	166		0.64±1.05	0.50±0.07	0.23±0.06	0.45±[0.2]
SCS	26 Jun 2014	0.79	2.2±1.4	15.1	11.3	4	0.8	13	9	32	0.07±0.05	0.47±0.27	0.05±0.003	35[1.7]
	17 Jul 2014	0.93	0.8±0.8	16.3	3.9	4	3.5	60	7		2.70±1.50	0.59±0.43	0.15	14[1.9]
	07 Aug 2014	0.75	2.2±1.0	14.1	7.2	6	2.2	49	12		1.32±1.19	0.89±0.25	0.77±0.22	1.6[0.3]
STN	24 Jun 2014	0.54	1.3±1.2	16.5	7.8	9	1.8	9	27	6.2	0.01±0.00	0.92±0.69	0.01	0.08[0.7]
	15 Jul 2014	0.59	1.4±1.4	20.1	8.5	9	1.5	2	21		0.68±1.17	0.49±0.19	0.16±0.04	0.26
	06 Aug 2014	0.60	1.4±1.7	15.5	8.5	11	1.8	12	8		0.34±0.17	0.93±0.10	0.28±0.06	0.70[0.2]
STS	24 Jun 2014	0.50	1.3±1.2	16.4	9.8	4	2.7	14	39	3.6	0.01±0.01	0.15±0.06	0.04±0.02	0.29
	15 Jul 2014	0.60	1.4±1.4	19.3	9.2	4	1.0	17	12		0.39±0.67	0.22±0.04	0.01	3.0[1.8]
	06 Aug 2014	0.61	1.4±1.7	14.5	9.0	4	1.0	18	45		0.08±0.15	0.28±0.11	0.02	6100[2.0]
TIN	26 Jun 2014	0.60	2.2±1.4	16.5	9.7	10	3.6	22	95	1.8	0.09±0.09	0.39±0.28	0.05±0.003	19[1.0]
	17 Jul 2014	0.62	0.8±0.8	18.3	5.6	19	4.2	44	24		3.54±2.89	0.19±0.05	ND	25[1.9]
	07 Aug 2014	0.74	2.2±1.0	16.3	8.0	34	2.1	30	16		0.82±0.83	0.27±0.10	0.05	2400[0.8]
TIS	26 Jun 2014	0.69	2.2±1.4	15.7	9.9	11	2.7	18	97	2.3	0.05±0.04	0.11±0.02	0.06	4.3[0.9]
	17 Jul 2014	0.76	0.8±0.8	18.1	7.1	26	2.1	32	24		1.27±0.75	0.12±0.03	0.02	8.1[0.6]
	07 Aug 2014	0.75	2.2±1.0	15.6	6.7	45	1.9	16	27		1.13±1.50	0.16±0.04	ND	4800[2.0]

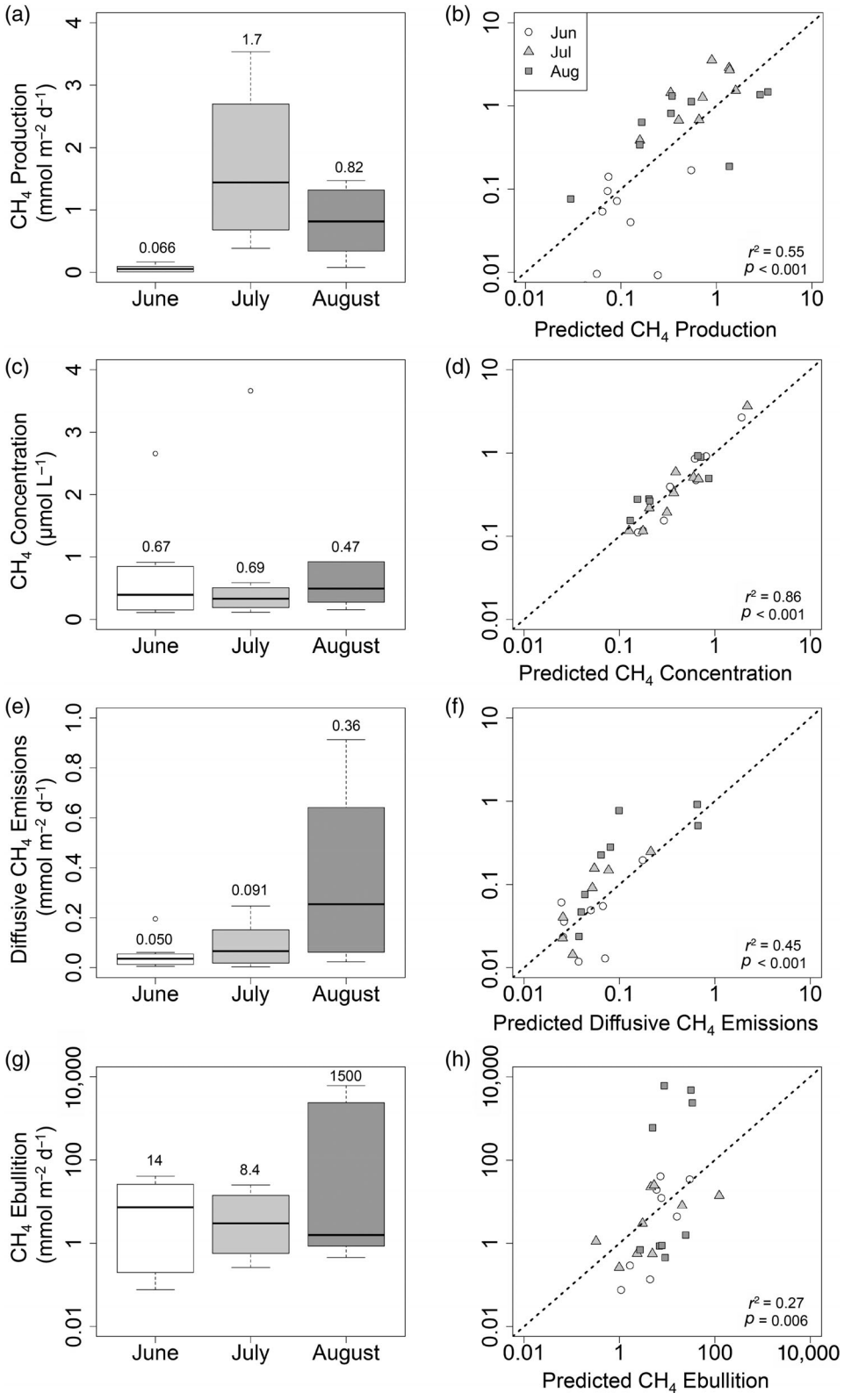

Fig. 1. Legend on next page.

Table 3. Best-fit models for CH_4 production, water-column CH_4 concentrations, diffusive emissions, and ebullition. DO in the lower water column, water-column Chl *a*, microbial community structure (*mcr* : *dsr*), water temperature (Temp), water-column CH_4 concentration [CH_4], and water depth were some of the potential parameters. Pseudo-r^2 after Nakagawa et al. (2017) was used to partition variance between the random and fixed effects. The hypothesis column indicates whether we predicted these factors would have a positive (+) or negative (−) effect (Fig. S1), and nonsignificant effects with a *p* value > 0.05 were marked "ns."

Response variable	# of observations	Random effect	Pseudo-r^2 (random/fixed)	Hypothesis	Parameter	Estimate	Standard error	*p*
$\log_{10}$ CH_4 production	27	Pond	0.02/0.49	−	DO	−0.143	0.043	0.004
				+	$\log_{10}$ Chl *a*	0.820	0.324	0.02
				+	$\log_{10}$ *mcr*:*dsr*	0.671	0.315	ns (0.07)
				+	Temp	0.148	0.076	ns (0.07)
					Intercept	−3.22	1.23	0.02
$\log_{10}$ CH_4 concentration	25	Pond	0.61/0.18	−	Depth	−1.52	0.58	0.02
					Intercept	0.558	0.388	ns (0.17)
$\log_{10}$ diffusive CH_4 emissions	25	Pond	0.04/0.38	+	[CH_4]	0.601	0.159	0.002
					Intercept	−1.06	0.12	<0.001
$\log_{10}$ CH_4 ebullition*	26	Pond	0.07/0.15	−	Depth	5.19	2.65	ns (0.07)
				+	Temp	−0.090	0.155	ns (0.57)
					Intercept	−1.09	1.66	ns (0.15)

*The best-fit model's residuals violated the assumption of normality (i.e., $\log_{10}$ CH_4 ebullition ~ depth), so we added an insignificant predictor variable back into the model (i.e., Temp) after Zuur et al. (2009).

wind speed, and DO) significantly enhanced fit during mixed-effect model selection, but DO was found in the next two best models with a $\Delta AIC_c < 0.3$ (Table S4).

Methane emissions

Diffusive CH_4 emission rates as assessed with flux chambers were highly variable (Table 2; Fig. 1e), and positively correlated with average water-column CH_4 concentrations. The best-fit model included pond as a random factor and average water-column CH_4 concentrations ($p = 0.002$) as a fixed effect (Table 3), which explained 4% and 38% of the variation in diffusive emissions, respectively. Although predictions were not as accurate for diffusive CH_4 emissions relative to production rates and water-column CH_4 concentrations, the best-fit line of the observed vs. predicted values did not statistically differ from the 1 : 1 line (i.e., H_0: slope = 1 and intercept = 0, $p > 0.7$ for both *t*-tests, df = 23; Fig. 1f). The inclusion of other physical and chemical variables—including DO, surface area, water depth, and wind speed—did not significantly enhance fit during mixed-effect model selection.

Additionally, we were able to balance pond CH_4 inputs and outputs across sampling intervals in most cases with 39–99% of the CH_4 produced being oxidized across these ponds using a budget approach (Table S3). This oxidation percentage was also strongly and positively correlated with the $\delta^{13}C$ of CH_4 in the lower water column ($p = 0.0008$; Fig. 2); pond as a random effect explained 6% of the variation, while $\delta^{13}C$ of CH_4 explained 75%.

Methane ebullition rates were challenging to predict. Some ponds exhibited higher ebullition rates at the August sampling event, but median ebullition rates were similar across sampling events (Table 2; Fig. 1g). The best-fit model complying with statistical assumptions included pond as a random effect and both water depth ($p = 0.07$) and water temperature ($p = 0.57$) as fixed effects (Table 3), which explained 7% and 15% of the variation, respectively. Water depth tended to have a positive, yet statistically insignificant, effect contrary to what we predicted (Fig. S1). The overall performance of the best-fit model was worse than other CH_4 dynamics, but the best-fit line of observed vs. predicted values did not differ significantly from the

Fig.1 Boxplots of (**a**) CH_4 production rates, (**c**) water-column CH_4 concentrations, (**e**) diffusive CH_4 emissions rates, and (**g**) CH_4 ebullition rates by sampling month. The boundaries of the box extend from the lower quartile to the upper quartile with the central dark line marking the median; the whiskers extend from the box to 1.5× the interquartile range unless no data points exceed 1.5× the interquartile range, in which case the whiskers represent either the minimum or maximum value. Mean values by sampling month are listed to two significant digits above each box. Methane ebullition rates were $\log_{10}$-transformed in g so that all observations could be visualized on the same plot. Predicted values from the best-fit model equations in Table 3 are compared to the actual values of (**b**) CH_4 production rates, (**d**) water-column CH_4 concentrations, (**f**) diffusive CH_4 emissions rates, and (**h**) CH_4 ebullition rates on $\log_{10}$ scales. In panels on the right, the dashed line represents the 1 : 1 line and the white circle = June, the gray triangle = July, and the gray square = August. The r^2 and *p* values are reported from the linear regression of observed vs. predicted values.

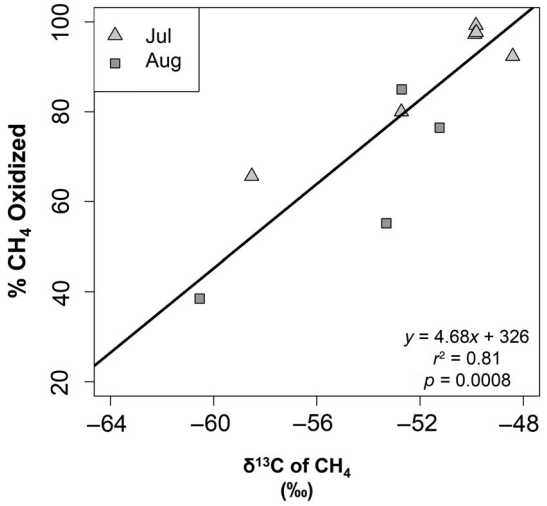

Fig. 2. Pond CH_4 oxidation rates (%) estimated with a mass balance equation plotted against the stable carbon isotope signatures ($\delta^{13}C$) of CH_4 measured in the lower water column just above the sediment. The solid line represents the equation from the linear regression where pond was included as a random factor. Specifically, June–July oxidation rates are plotted vs. July $\delta^{13}CH_4$ and July–August oxidation rates vs. August $\delta^{13}CH_4$. Site replicates ($n = 2$) from a single pond and sampling event were averaged if these data existed, and $\delta^{13}C$ of CH_4 values were not included in this plot without a corresponding oxidation estimate (Table S3); six ponds are represented.

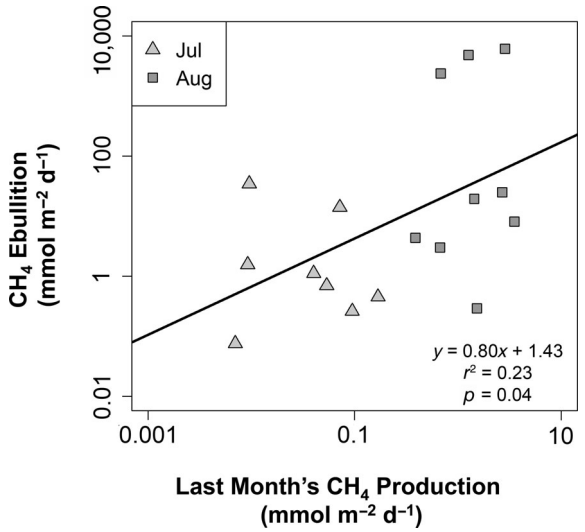

Fig. 3. Methane ebullition rates from July and August are plotted against the previous month's CH_4 production rates (i.e., June and July, respectively). The solid line represents the equation from their linear regression where pond was included as a random factor, but explained less than 1% of the variation. All nine ponds are represented here for both sampling periods except for Eyak N where we only detected ebullition in August.

1 : 1 line (i.e., H_0: slope = 1 and intercept = 0, $p = 0.5$ for both t-tests, df = 24; Fig. 1h). Methane production rates and wind speed were also considered in model selection, but they did not significantly enhance fit.

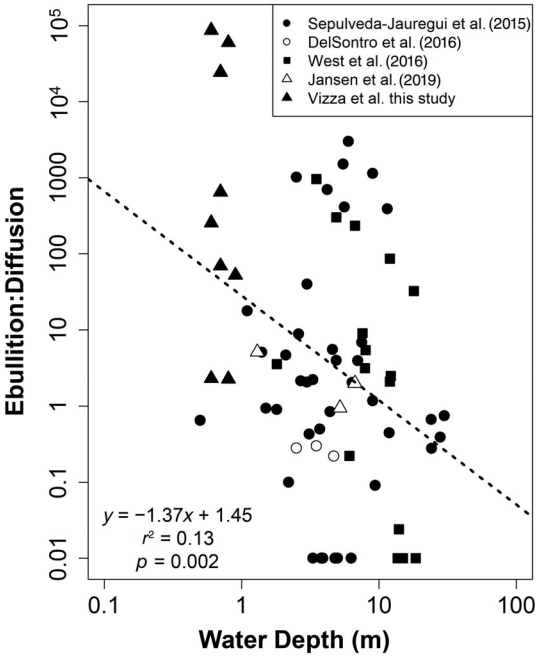

Fig. 4. The ratio of ebullition to diffusive emissions from northern lakes and ponds ($n = 71$) plotted against water depth; both variables were $\log_{10}$-transformed. The dotted line represents the equation from their linear regression where study was also included as a random factor, but explained less than 1% of the variation. Maximum depth was plotted for all studies except for DelSontro et al. (2016) where only mean depth was available.

Because it is possible that bubbles were integrating sources of CH_4 over longer time scales than our incubations, we also examined the effect of CH_4 production rates from the previous sampling event on July and August ebullition rates (Fig. 3). When pond was included as a random factor, the previous month's production ($p = 0.04$) explained about 1.5× more variation (i.e., 23%) in ebullition than water depth and water temperature together (i.e., 15%).

Ratio of ebullition to diffusive CH_4 emissions

The ratio of ebullition to diffusive CH_4 emissions was generally high in these Alaskan ponds (range: 2.3–87,000, median = 260). When we examined this ratio in the four other studies in northern lakes, we found that water depth had a significant, negative effect ($p = 0.002$; Fig. 4), but area was not significant ($p > 0.5$). Study as a random factor explained less than 1% of the variation in the ratio of ebullition to diffusive CH_4 emissions, while depth explained 13%. In the subset of studies with water chemistry data, the best-fit model included study as a random factor, which explained less than 1% of the variation, and mean depth and Chl *a* as fixed effects. Depth had a significant, negative effect ($p = 0.0008$) and Chl *a* had a significant, positive effect ($p = 0.03$), which together explained 48% of the variation in the ratio of ebullition to diffusive CH_4 emissions. Area,

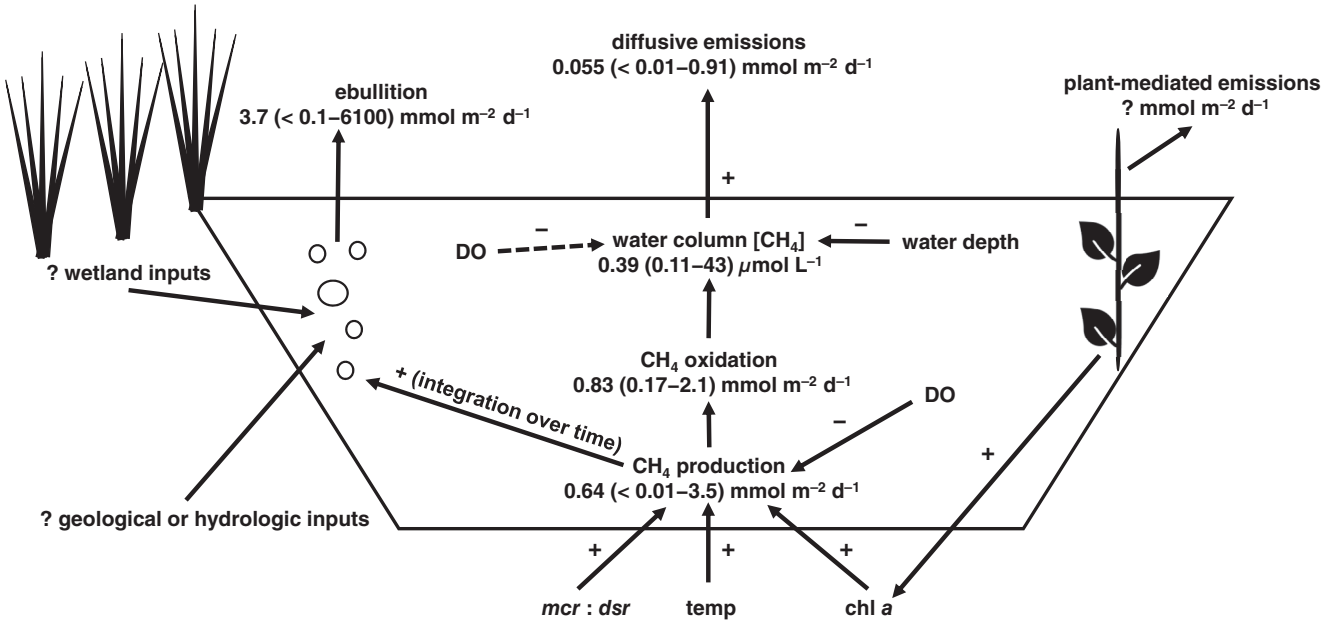

Fig. 5. Conceptual diagram of the CH_4 cycling dynamics observed in Alaskan ponds. A pond is represented by a trapezoid. Solid arrows depict a direct effect, while a dashed arrow depicts an indirect effect. Positive (+) and negative (−) signs indicate the direction of the effect observed with best mixed-effect models (Table 3). The median of all observations is reported for each estimate along with the range in parentheses. Oxidation rates were estimated using a mass balance equation. "?" indicates no direct measurement of this process. Chl a = chlorophyll a, DO = dissolved oxygen, mcr:dsr = the ratio of methanogens relative to sulfate-reducers, and temp = water temperature.

dissolved organic carbon, and total phosphorus did not significantly enhance the fit of the model, and there was no other model within $\Delta AIC_c < 2$.

Discussion

We conducted a cross-scale exploration of the CH_4 dynamics from microbe to ecosystem budget (Fig. 5), including measuring CH_4 production in conjunction with emissions, which is rare in many of the previous studies in lakes or ponds (but see Huttunen et al. 2006; West et al. 2016; Aguirrezabala-Campano et al. 2021). By exploiting the spatial and temporal heterogeneity of CH_4 dynamics in these Alaskan ponds, our study also identified important biological, physical, and chemical factors. Specifically, pond CH_4 production was influenced by DO, Chl *a*, and microbial communities, while average water-column CH_4 concentrations varied across ponds by total pond depth and DO levels, and diffusive emissions assessed with flux chambers were directly related to water-column CH_4 concentrations. We also observed a strong relationship between oxidation estimates calculated from a mass balance equation and water-column $\delta^{13}CH_4$ (Fig. 2), suggesting that dissolved CH_4 dynamics across the summer in these ponds can indeed be explained with a budget approach, which is even more compelling considering the study's low temporal resolution.

CH_4 dynamics across the summer

Interestingly, CH_4 production peaked in July, while CH_4 diffusive emissions and ebullition peaked in August suggesting high oxidation rates in July and perhaps a delayed release of bubbles, respectively. We have previously hypothesized that CH_4 production is low early in the growing season when less organic matter (i.e., Chl *a*; Table 2) is available, then reaches its maximum during peak growing season (Fig. 1a) when labile plant exudates are abundant (Vizza et al. 2017a). We also observed the highest sulfate availability in June (Table 2) suggesting that competition with sulfate-reducers may be greatest earlier in the summer. This trend is also supported by an osmosampler study conducted in two of the same Alaskan ponds over the period of a year, which revealed that increases in pore-water CH_4 concentrations tended to lag behind the decrease in pore-water sulfate early in the summer (J. Buser, unpubl. data), thus supporting the idea that seasonal fluctuations in redox conditions and microbial community activity do occur even over a few months.

Despite observing the highest rates of CH_4 production in July (Fig. 1a), July oxidation rates were likely also high resulting in lower emissions (Fig. 2; Table 2). Then as the plants started to senesce around August, more organic matter was available, and oxygen levels remained lower than their peak in June (Table 2), which resulted in generally higher water-column CH_4 concentrations, diffusive CH_4 emissions, and ebullition in August (Fig. 1). Methane production in these Alaskan ponds may remain high early in fall until colder temperatures drive down microbial processing rates (Lofton et al. 2014). We hypothesize that macrophyte phenology influences the availability of organic matter and electron acceptors (Lyautey et al. 2021), which ultimately

drive the temporal differences in microbial activity, while the fate of CH_4 in these Alaskan ponds appears to be largely driven by physical and chemical factors (Vachon et al. 2019).

Methane production is shaped by physical, chemical, and biological factors

Methane production can be challenging to measure in situ. For example, while CH_4 concentrations can be measured in the pore water using osmosamplers on site, these data reflect both CH_4 production and oxidation. One of the most widely used methods to estimate production involves anoxic incubations of sediment or slurries in the dark. The rates from these incubations are generally considered to be production potentials because they are not conducted at in situ temperature and light levels. Additionally, the possibility of some anaerobic CH_4 oxidation when manganese, iron, or sulfate is present cannot be ruled out. In light of these limitations, our CH_4 production rates are likely underestimates, but relative comparisons of these rates can still be illuminating.

Methane production rates in these Alaskan ponds were most influenced by DO levels followed by biological factors and then temperature. In light of the incubations being anoxic and held at a relatively constant temperature, DO and temperature do not actually represent conditions experienced in the incubations, but may instead be capturing temporal variation in the availability of organic matter and electron acceptors associated with macrophyte phenology (Lyautey et al. 2021; see the CH_4 dynamics across the summer section above). Additionally, microbial community structure played a role whereby methanogens, the microbial organisms responsible for CH_4 production, can be outcompeted for organic matter substrates by other microbial organisms (e.g., sulfate-reducers) when alternate electron acceptors like sulfate are readily available (Lovley and Klug 1983; Lovley and Phillips 1987). Therefore, higher *mcr* : *dsr* likely indicates better habitat suitability at the sediment–water interface for methanogens relative to their competitors, sulfate-reducers. While some studies examine methanogen community structure (Matheus Carnevali et al. 2018; Kadnikov et al. 2019), very few simultaneously measure CH_4 production and microbial community composition (but see Heslop et al. 2019). This direct link between CH_4 production estimates in our ponds and the relative abundance of methanogens to sulfate-reducers suggests that microbial community structure and their competitive interactions directly impact ecosystem function across these Alaskan ponds; *mcr* : *dsr* could therefore be a potential tool for understanding CH_4 dynamics in ecosystems near the coast or with high sulfate availability.

Pond CH_4 production estimates were likely influenced by an indicator of primary productivity (i.e., Chl *a*). This finding is consistent with research in northern Wisconsin lakes that Chl *a* was correlated with total CH_4 production (West et al. 2016), which is fueled by high-quality autochthonous sources (West et al. 2012, 2015). While this study did not directly examine the effect of substrate quality, we have previously observed that the addition of only some macrophyte species enhanced CH_4 production in these ponds (Vizza et al. 2017a). Macrophyte stoichiometry (i.e., ratios of carbon to nitrogen or phosphorus) can influence CH_4 production (Grasset et al. 2019), but so can specific compounds. For example, in a Canadian boreal lake, Emilson et al. (2018) demonstrated that phenol availability, which was lower in aquatic relative to terrestrial litter, regulated CH_4 production. As tissue stoichiometry did not appear to responsible, phenol inhibition could be a plausible mechanism for explaining why only a subset of aquatic vegetation species enhanced CH_4 production in these ponds (Vizza et al. 2017a). Models that use organic matter quality and quantity to predict CH_4 production (Grasset et al. 2021) could therefore be useful in reducing uncertainty in the freshwater CH_4 budget.

Methane concentrations are influenced by water depth and a pond's DO levels

While physical and chemical factors tended to influence water-column CH_4 concentrations, the spatial heterogeneity of these ponds that we were unable to capture with our measurements was most influential. Even across a small range (0.4–0.9 m), depth was still negatively correlated with mean water-column CH_4 concentrations across these Alaskan ponds. Deeper systems tend to have larger water volumes, which can dilute CH_4 but also lead to higher rates of CH_4 oxidation by increasing CH_4's exposure to oxygen in the water column (Bastviken et al. 2004, 2008). Pond as a random factor ($n = 9$) explained most of the variation in CH_4 concentrations, but if removed, DO had a statistically significant, negative effect on CH_4. Together, depth and DO could explain 35% of the variation in CH_4 concentrations, which about doubles the percentage explained by fixed effects in the best-fit model. This trend suggests that DO may influence how much CH_4 is removed from the water as previously seen in shallow Alaskan lakes (Lofton et al. 2014). Additionally, Sepulveda-Jauregui et al. (2015) showed the summer CH_4 concentrations in Alaskan lakes were inversely related to DO levels in the lower water column; their highest CH_4 concentrations were at least an order of magnitude higher (~ 60–800 μmol L^{-1}) when DO rose above 2 mg L^{-1} than our Alaskan ponds, with their top three lakes ranging from 3.3–6 m in maximum depth. Therefore, depth and DO influence water-column CH_4 concentrations by shaping the microbial processes that consume CH_4 in both shallow and deep aquatic ecosystems.

Pond CH_4 oxidation estimates are comparable to those in deeper lakes

Because oxidation percentages were highly correlated with $\delta^{13}CH_4$ in the lower water column (Fig. 2), we believe that dissolved CH_4 dynamics across the summer in these ponds can indeed be explained with a budget approach. The percentage of CH_4 produced that was oxidized in the water column ranged from 39% to 99% (Table S3), which is comparable to

the 22–100% observed by Bastviken et al. (2008) across all layers in three lakes in the northern United States (3.7–5.7 m mean depth), the 24–64% observed by Jansen et al. (2019) in three Swedish lakes (1.1–6.7 m maximum depth), and the 91% observed by Saarela et al. (2019) in a boreal lake in Finland (13 m maximum depth). This similarity may be surprising in light of the greater depths of most of those lakes. However, any hydrologic or other external inputs of CH_4 would result in underestimating, not overestimating, oxidation with our mass balance approach. Perhaps what matters most is the degree of stratification and how dramatic the oxycline, or the change in DO with depth. For example, DO decreased at a rate of around 1 mg L^{-1} m^{-1} when the hypolimnion was most hypoxic and the greatest oxidation was observed in a deep Finland lake (Saarela et al. 2019), whereas our ponds averaged 3 mg L^{-1} m^{-1} across all ponds and sampling events (Table S2). Therefore, we hypothesize that a large percentage of CH_4 produced may be oxidized in shallow ecosystems especially if there is a dramatic change in oxygen levels at the sediment–water interface where most CH_4 is oxidized (Whalen 2005).

Diffusive CH_4 emissions and ebullition are driven by other CH_4 dynamics

Our best-fit model did a reasonable job of predicting diffusive emissions for such a heterogeneous landscape as the Copper River Delta (Vizza et al. 2017b). Specifically, average water-column CH_4 concentrations were the most important predictor of pond diffusive CH_4 emissions as assessed with flux chambers. We expected this pattern because many studies using Fick's law of diffusion to directly estimate diffusive emissions from water-column CH_4 concentrations (Huttunen et al. 2006; Juutinen et al. 2009; Matveev et al. 2016). However, quantifying the gas transfer coefficient at the air–water interface is complicated when considering turbulence and stratification of aquatic ecosystems (MacIntyre et al. 2010; MacIntyre et al. 2018).

However, ebullition can be difficult to predict due to spatial and temporal heterogeneity, with estimates varying by several orders of magnitude in these Alaskan ponds as well as in Alaskan and Siberian lakes (Walter Anthony et al. 2010). While DelSontro et al. (2016) found that CH_4 ebullition in Québec lakes and ponds was regulated by the interaction of ecosystem productivity and sediment temperature, Burke et al. (2019) found very weak correlations with environmental variables and their high-frequency ebullition measurements ($n = 2063$) in eight small thaw ponds in Sweden. Similarly, our best-fit model in Table 3 failed to provide additional mechanistic understanding of ebullition. However, we were able to explain about a quarter of the variation in ebullition by the previous month's CH_4 production suggesting that bubbles integrate CH_4 sources over at least a month in these ponds, which makes sense when one considers how bubbles are formed and released (Peltola et al. 2018). Models of the physical process of ebullition often use a threshold-based approach for CH_4 porewater concentration, pressure, or bubble volume (Peltola et al. 2018). Therefore, CH_4 in gaseous form could accumulate in the pore spaces of sediment for a period longer than a few weeks before it reaches the threshold necessary for emission to the atmosphere; these events can often be triggered by fluctuations in atmospheric pressure (Tokida et al. 2007; Zhao et al. 2021).

What are the potential sources of CH_4 ebullition in these Alaskan ponds?

Despite the low temporal resolution of our measurements, which has been reasonably criticized by Wik et al. (2016a) as problematic for extrapolation to global CH_4 budgets, it is still worth noting that daily ebullition rates exceeded daily production estimates in 70% of the pond sampling events (Table 2). Although Wilkinson et al. (2015), found that sediment CH_4 bubble formation was dominant at 0.14–0.2 m in depth, Liu et al. (2016) observed a similar pattern for active bubble formation, but the active depth varied by sediment type. Even if we scale up production estimates based on an active depth of 1 m instead of 0.2 m and use the highest Q_{10} estimate (i.e., 12) from Bergman et al. (2000) to account for the incubation temperatures being lower than those of the ponds, ebullition still exceeded these scaled-up production estimates in 41% of the events. If we go further and assume that a day's ebullition is reflective of 2 weeks of scaled-up production estimates, a single sampling event's daily ebullition rate still exceeds these 2-week production estimates in 30% of the pond sampling events. In comparison, Scandella et al. (2017) observed that bubble outlets, or ebullition hotspots, in sediments can demonstrate activity for a few days to even months. Our scale-up comparisons along with the decent relationship between ebullition and the previous month's production (Fig. 3) suggests that the bubbles in these ponds, at the very least during our sampling events, can integrate sources of CH_4 over a month or more.

While the ability of bubbles to integrate older sources of CH_4 has been observed in arctic lakes (Walter et al. 2008), our study ponds are located in the temperate zone of Alaska, which has glaciers but lacks permafrost. Since glacial carbon has a distinct radiocarbon signature ($^{14}C/^{12}C$) from contemporary primary production (Fellman et al. 2015), the possibility that glacial carbon fuels ebullition could be investigated by capturing bubbles after Walter et al. (2008) and comparing their radiocarbon signatures to that of aquatic/wetland primary producers, pond sediments at different depths, and glacial sediments.

Alternate sources of CH_4 bubbles could include hydrologic or geological inputs, but we think these inputs are unlikely for these Alaskan ponds. For some aquatic systems, hydrologic inputs can affect CH_4 dynamics, especially in areas with permafrost (Paytan et al. 2015; Kohnert et al. 2017). Although we assumed minimal hydrologic inputs to estimate

oxidation rates, the strong relationship between oxidation estimates and water-column $\delta^{13}CH_4$ would be even more unlikely if that assumption were violated. Additionally, hydrologic inputs from surface runoff or groundwater are likely to contribute to dissolved CH_4, not bubbles. However, it should be noted that geological sources of CH_4 can seep out along fault lines in southcentral Alaska (Walter Anthony et al. 2012), which may contribute to ebullition in these ponds. Because $\delta^{13}C$ of CH_4 from geological sources tends to be more enriched (i.e., −40‰ to −20‰) than what we observed (Whiticar 1999), we think that biogenic sources from nearby wetlands are more likely to contribute to bubbles than geological sources.

Lateral clustering and transport of CH_4 bubbles (Scandella et al. 2017) from the wetland fringes may contribute to high ebullition rates in these systems. Bubbles could be trapped under the vegetation mats that fringe these ponds gradually traveling towards open water where they can be emitted following a drop in hydrostatic pressure (Scandella et al. 2017). Most of the ponds have a large *Sphagnum*/wetland fringe, especially the systems where we observed some of the highest ebullition rates (i.e., EYN, TIN, and TIS; Table 2). Even though flux samples were collected by raft, it is possible that we inadvertently increased these lateral inputs by traversing the wetland fringe to access the pond. To truly tease apart whether the source of these bubbles is from geological seeps or the surrounding wetlands, ^{14}C of the bubbles should be measured after Walter Anthony et al. (2012). Additionally, we did not include decomposing macrophyte tissue in our sediment slurry incubations, but we have previously shown that the addition of some macrophytes species can enhance CH_4 production (Vizza et al. 2017a). Decomposition of macrophytes could contribute the CH_4 that is emitted by ebullition. While we may be unsure of the exact source of these high ebullition rates, this process is fueled by CH_4 sources other than pond production rates from a single sampling event alone.

The ratio of diffusive CH_4 emissions to ebullition across northern ponds and lakes

While diffusive CH_4 emissions in these Alaskan ponds were relatively modest, ebullition dominated fluxes in comparison to northern lakes. Average and interquartile range of our pond diffusive emission means (0.15, 0.05–0.22 mmol m^{-2} d^{-1}) were much lower than those from 73 glacial/post-glacial lakes (0.8, 0.2–1.1 mmol m^{-2} d^{-1}) and 70 thermokarst waterbodies (2.1, 0.2–2.4 mmol m^{-2} d^{-1}), which were measured during ice-off periods and compiled in Wik et al. (2016b). While high ebullition rates up to 1500 mmol m^{-2} d^{-1} have been captured in Siberian and Alaskan lake seeps identified with ice-bubble classification (Walter Anthony et al. 2010), northern lakes generally exhibited lower ebullition rates than those in these Alaskan ponds. For example, average ebullition rates along with their interquartile ranges for 29 glacial/post-glacial lakes (2.0, 0.6–3.6 mmol m^{-2} d^{-1}) and 18 thermokarst waterbodies (5.5, 0.4–8.2 mmol m^{-2} d^{-1}; Wik et al. 2016b) were much lower than in the nine Alaskan ponds in this study (520, 12–810 mmol m^{-2} d^{-1}). In contrast to the deeper, northern waterbodies in Wik et al. (2016b), fluxes from these Alaskan ponds were more dominated by ebullition relative to diffusion.

To our knowledge, a systematic comparison of ebullition to diffusive CH_4 emissions has not been conducted. Using data from our Alaskan ponds and other northern lakes (Sepulveda-Jauregui et al. 2015; DelSontro et al. 2016; West et al. 2016; Jansen et al. 2019), we established that the ratio of ebullition to diffusive CH_4 emissions tends to be larger in shallower aquatic ecosystems (Fig. 4), which supports the finding that depth influences ebullition (DelSontro et al. 2016; West et al. 2016). However, when we examine the ratio of ebullition to diffusive CH_4 emissions in our ponds alone, maximum depth only ranges from 0.6 to 0.9 m and is not a good predictor, but Chl *a* explains a little more than 20% of the variability in the log-transformed ratio of these emission pathways. Interestingly, Chl *a*, an indicator of productivity, also had a positive effect on the ratio of ebullition to diffusive CH_4 emissions across studies, while total phosphorus or CH_4 production were the positive predictors of ebullition in DelSontro et al. (2016) and West et al. (2016), respectively. Deemer and Holgerson (2021) also found that Chl *a* was the best predictor of ebullition in 130 lakes and reservoirs. Together these findings suggest that indicators of ecosystem productivity influence the pathways of CH_4 emissions.

Conclusion

Our study examined potential physical, chemical, and biological factors that influence CH_4 production, water-column CH_4 concentrations, diffusive emissions, and ebullition in nine Alaskan ponds during summer. While pond CH_4 dynamics were generally similar to those observed in northern lakes, pond ebullition played a significantly larger role than diffusive emissions with even greater ebullition rates than most of those previously observed in northern lakes (Wik et al. 2016b). Pond ebullition rates often exceeded our CH_4 production estimates even when scaled up to account for methodological limitations (i.e., active depth assumption, lower incubation temperature, and the likelihood that ebullition rates integrate production over comparatively longer time frames), which suggests that CH_4 bubbles may integrate sources over a month and/or across the wetlands fringing a pond. Our study demonstrates that ignoring ebullition from ponds and other productive, shallow ecosystems would greatly underestimate their importance to the freshwater CH_4 budget.

Data availability statement

Data will be accessible at https://knb.ecoinformatics.org doi:10.5063/F1CZ35MS.

References

Aguirrezabala-Campano, T., R. Gonzalez-Valencia, F. J. Cervantes, and F. Thalasso. 2021. Overall spatiotemporal dynamics of greenhouse gasses and oxygen in two subtropical reservoirs with contrasting trophic states. Water Res. **196**: 117056. doi:10.1016/j.watres.2021.117056

Banning, N., F. Brock, J. C. Fry, R. J. Parkes, E. R. C. Hornibrook, and A. J. Weightman. 2005. Investigation of the methanogen population structure and activity in a brackish lake sediment. Environ. Microbiol. **7**: 947–960. doi:10.1111/j.1462-2920.2004.00766.x

Barbosa, P. M., J. M. Melack, J. H. F. Amaral, A. Linkhorst, and B. R. Forsberg. 2021. Large seasonal and habitat differences in methane ebullition on the Amazon floodplain. J. Geophys. Res. Biogeosci. **126**: e2020JG005911. doi:10.1029/2020JG005911

Bastviken, D., J. J. Cole, M. L. Pace, and M. C. Van de Bogert. 2008. Fates of methane from different lake habitats: Connecting whole-lake budgets and CH_4 emissions. J. Geophys. Res. Biogeo. **113**: G02024. doi:10.1029/2007JG000608

Bastviken, D., J. Cole, M. Pace, and L. Tranvik. 2004. Methane emissions from lakes: Dependence of lake characteristics, two regional assessments, and a global estimate. Global Biogeochem. Cycles **18**: GB4009. doi:10.1029/2004GB002238

Bastviken, D., J. Ejlertsson, and L. Tranvik. 2002*a*. Measurement of methane oxidation in lakes: A comparison of methods. Environ. Sci. Technol. **36**: 3354–3361. doi:10.1021/es010311p

Bastviken, D., J. Ejlertsson, and L. Tranvik. 2002*b*. Measurement of methane oxidation in lakes: A comparison of methods. Environ. Sci. Technol. **36**: 3354–3361. doi:10.1021/es010311p

Bergman, I., M. Klarqvist, and M. Nilsson. 2000. Seasonal variation in rates of methane production from peat of various botanical origins: Effects of temperature and substrate quality. FEMS Microbiol. Ecol. **33**: 181–189. doi:10.1111/j.1574-6941.2000.tb00740.x

Bertolet, B. L., W. E. West, D. W. Armitage, and S. E. Jones. 2019. Organic matter supply and bacterial community composition predict methanogenesis rates in temperate lake sediments. Limnol. Oceanogr. Lett. **4**: 164–172. doi:10.1002/lol2.10114

Bryant, M. D. 1991. The Copper River Delta pulse study: an interdisciplinary survey of aquatic habitats. General Technical Report PNW-GTR-282. PNW-GTR-282 U.S.D.A., Forest Service, Pacific Northwest Research Station.

Burke, S. A., M. Wik, A. Lang, A. R. Contosta, M. Palace, P. M. Crill, and R. K. Varner. 2019. Long-term measurements of methane ebullition from thaw ponds. J. Geophys. Res. Biogeo. **124**: 2208–2221. doi:10.1029/2018JG004786

Castro, H., A. Ogram, and K. R. Reddy. 2004. Phylogenetic characterization of methanogenic assemblages in eutrophic and oligotrophic areas of the Florida Everglades. Appl. Environ. Microbiol. **70**: 6559–6568. doi:10.1128/AEM.70.11.6559-6568.2004

Cole, J. J., D. L. Bade, D. Bastviken, M. L. Pace, and M. Van de Bogert. 2010. Multiple approaches to estimating air-water gas exchange in small lakes. Limnol. Oceanogr.: Methods **8**: 285–293. doi:10.4319/lom.2010.8.285

Cole, J. J., and N. F. Caraco. 1998. Atmospheric exchange of carbon dioxide in a low-wind oligotrophic lake measured by the addition of SF6. Limnol. Oceanogr. **43**: 647–656. doi:10.4319/lo.1998.43.4.0647

Deemer, B. R., and M. A. Holgerson. 2021. Drivers of methane flux differ between lakes and reservoirs, complicating global upscaling efforts. J. Geophys. Res. Biogeosci. **126**: e2019JG005600. doi:10.1029/2019JG005600

DelSontro, T., L. Boutet, A. St-Pierre, P. A. del Giorgio, and Y. T. Prairie. 2016. Methane ebullition and diffusion from northern ponds and lakes regulated by the interaction between temperature and system productivity. Limnol. Oceanogr. **61**: S62–S77. doi:10.1002/lno.10335

Earl, J., G. Hall, R. W. Pickup, D. A. Ritchie, and C. Edwards. 2003. Analysis of methanogen diversity in a hypereutrophic lake using PCR-RFLP analysis of mcr sequences. Microb. Ecol. **46**: 270–278. doi:10.1007/s00248-003-2003-x

Emilson, E. J. S., and others. 2018. Climate-driven shifts in sediment chemistry enhance methane production in northern lakes. Nat. Commun. **9**: 1801. doi:10.1038/s41467-018-04236-2

Fellman, J. B., E. Hood, P. A. Raymond, J. Hudson, M. Bozeman, and M. Arimitsu. 2015. Evidence for the assimilation of ancient glacier organic carbon in a proglacial stream food web. Limnol. Oceanogr. **60**: 1118–1128. doi:10.1002/lno.10088

Grasset, C., G. Abril, R. Mendonça, F. Roland, and S. Sobek. 2019. The transformation of macrophyte-derived organic matter to methane relates to plant water and nutrient contents. Limnol. Oceanogr. **64**: 1737–1749. doi:10.1002/lno.11148

Grasset, C., R. Mendonça, G. V. Saucedo, D. Bastviken, F. Roland, and S. Sobek. 2018. Large but variable methane production in anoxic freshwater sediment upon addition of allochthonous and autochthonous organic matter. Limnol. Oceanogr. **63**: 1488–1501. doi:10.1002/lno.10786

Grasset, C., S. Moras, A. Isidorova, R.-M. Couture, A. Linkhorst, and S. Sobek. 2021. An empirical model to predict methane production in inland water sediment from particular organic matter supply and reactivity. Limnol. Oceanogr. **66**: 3643–3655. doi:10.1002/lno.11905

Griffiths, R. P., B. A. Caldwell, J. D. Cline, W. A. Broich, and R. Y. Morita. 1982. Field observations of methane concentrations and oxidation rates in the southeastern Bering Sea. Appl. Environ. Microbiol. **44**: 435–446.

Heslop, J. K., K. M. Walter Anthony, G. Grosse, S. Liebner, and M. Winkel. 2019. Century-scale time since permafrost thaw

affects temperature sensitivity of net methane production in thermokarst-lake and talik sediments. Sci. Total Environ. **691**: 124–134. doi:10.1016/j.scitotenv.2019.06.402

Holgerson, M. A., and P. A. Raymond. 2016. Large contribution to inland water CO_2 and CH_4 emissions from very small ponds. Nat. Geosci. **9**: 222–226. doi:10.1038/ngeo2654

Huttunen, J. T., P. J. Martikainen, T. S. Vaeisaenen, and S. K. Hellsten. 2006. Methane fluxes at the sediment-water interface in some boreal lakes and reservoirs. Boreal Environ. Res. **11**: 27–34.

Jansen, J., B. F. Thornton, M. M. Jammet, M. Wik, A. Cortés, T. Friborg, S. MacIntyre, and P. M. Crill. 2019. Climate-sensitive controls on large spring emissions of CH_4 and CO_2 from northern lakes. J. Geophys. Res. Biogeo. **124**: 2379–2399. doi:10.1029/2019JG005094

Juutinen, S., J. Alm, T. Larmola, J. T. Huttunen, M. Morero, P. J. Martikainen, and J. Silvola. 2003. Major implication of the littoral zone for methane release from boreal lakes. Global Biogeochem. Cycles **17**: 1117. doi:10.1029/2003GB002105

Juutinen, S., M. Rantakari, P. Kortelainen, J. T. Huttunen, T. Larmola, J. Alm, J. Silvola, and P. J. Martikainen. 2009. Methane dynamics in different boreal lake types. Biogeosciences **6**: 209–223. doi:10.5194/bg-6-209-2009

Kadnikov, V. V., A. S. Savvichev, A. V. Mardanov, A. V. Beletsky, A. Y. Merkel, N. V. Ravin, and N. V. Pimenov. 2019. Microbial communities involved in the methane cycle in the near-bottom water layer and sediments of the meromictic subarctic Lake Svetloe. Antonie Van Leeuwenhoek **112**: 1801–1814. doi:10.1007/s10482-019-01308-1

Kelly, C. A., and D. P. Chynoweth. 1981. The contributions of temperature and of the input of organic matter in controlling rates of sediment methanogenesis. Limnol. Oceanogr. **26**: 891–897. doi:10.4319/lo.1981.26.5.0891

Klein, M., and others. 2001. Multiple lateral transfers of dissimilatory sulfite reductase genes between major lineages of sulfate-reducing prokaryotes. J. Bacteriol. **183**: 6028–6035. doi:10.1128/JB.183.20.6028-6035.2001

Kohnert, K., A. Serafimovich, S. Metzger, J. Hartmann, and T. Sachs. 2017. Strong geologic methane emissions from discontinuous terrestrial permafrost in the Mackenzie Delta, Canada. Sci. Rep. **7**: 1–6. doi:10.1038/s41598-017-05783-2

Kritzberg, E. S., J. J. Cole, M. L. Pace, W. Granéli, and D. L. Bade. 2004. Autochthonous versus allochthonous carbon sources of bacteria: Results from whole-lake ^{13}C addition experiments. Limnol. Oceanogr. **49**: 588–596. doi:10.4319/lo.2004.49.2.0588

Liu, L., J. Wilkinson, K. Koca, C. Buchmann, and A. Lorke. 2016. The role of sediment structure in gas bubble storage and release. J. Geophys. Res. Biogeo. **121**: 1992–2005. doi:10.1002/2016JG003456

Lofton, D. D., S. C. Whalen, and A. E. Hershey. 2014. Effect of temperature on methane dynamics and evaluation of methane oxidation kinetics in shallow Arctic Alaskan lakes. Hydrobiologia **721**: 209–222. doi:10.1007/s10750-013-1663-x

Lovley, D. R., and M. J. Klug. 1983. Sulfate reducers can outcompete methanogens at freshwater sulfate concentrations. Appl. Environ. Microbiol. **45**: 187–192.

Lovley, D. R., and E. J. P. Phillips. 1987. Competitive mechanisms for inhibition of sulfate reduction and methane production in the zone of ferric iron reduction in sediments. Appl. Environ. Microbiol. **53**: 2636–2641.

Luton, P. E., J. M. Wayne, R. J. Sharp, and P. W. Riley. 2002. The mcrA gene as an alternative to 16S rRNA in the phylogenetic analysis of methanogen populations in landfill. Microbiology **148**: 3521–3530. doi:10.1099/00221287-148-11-3521

Lyautey, E., E. Billard, N. Tissot, S. Jacquet, and I. Domaizon. 2021. Seasonal dynamics of abundance, structure, and diversity of methanogens and methanotrophs in lake sediments. Microb. Ecol. **82**: 559–571. doi:10.1007/s00248-021-01689-9

MacIntyre, S., and others. 2021. Turbulence in a small boreal lake: Consequences for air–water gas exchange. Limnol. Oceanogr. **66**: 827–854. doi:10.1002/lno.11645

MacIntyre, S., A. T. Crowe, A. Cortés, and L. Arneborg. 2018. Turbulence in a small arctic pond. Limnol. Oceanogr. **63**: 2337–2358. doi:10.1002/lno.10941

MacIntyre, S., A. Jonsson, M. Jansson, J. Aberg, D. E. Turney, and S. D. Miller. 2010. Buoyancy flux, turbulence, and the gas transfer coefficient in a stratified lake. Geophys. Res. Lett. **37**: L24604. doi:10.1029/2010GL044164

Matheus Carnevali, P. B., C. W. Herbold, K. P. Hand, J. C. Priscu, and A. E. Murray. 2018. Distinct microbial assemblage structure and archaeal diversity in sediments of Arctic thermokarst lakes differing in methane sources. Front. Microbiol. **9**: 1192. doi:10.3389/fmicb.2018.01192

Matthews, C. J. D., V. L. St. Louis, and R. H. Hesslein. 2003. Comparison of three techniques used to measure diffusive gas exchange from sheltered aquatic surfaces. Environ. Sci. Technol. **37**: 772–780. doi:10.1021/es0205838

Matveev, A., I. Laurion, B. N. Deshpande, N. Bhiry, and W. F. Vincent. 2016. High methane emissions from thermokarst lakes in subarctic peatlands. Limnol. Oceanogr. **61**: S150–S164. doi:10.1002/lno.10311

Nakagawa, S., P. C. D. Johnson, and H. Schielzeth. 2017. The coefficient of determination R^2 and intra-class correlation coefficient from generalized linear mixed-effects models revisited and expanded. J. R. Soc. Interface **14**: 20170213. doi:10.1098/rsif.2017.0213

Paytan, A., A. L. Lecher, N. Dimova, K. J. Sparrow, F. G.-T. Kodovska, J. Murray, S. Tulaczyk, and J. D. Kessler. 2015. Methane transport from the active layer to lakes in the Arctic using Toolik Lake, Alaska, as a case study. Proc. Natl. Acad. Sci. **112**: 3636–3640. doi:10.1073/pnas.1417392112

Peltola, O., M. Raivonen, X. Li, and T. Vesala. 2018. Technical note: Comparison of methane ebullition modelling

approaches used in terrestrial wetland models. Biogeosciences **15**: 937–951. doi:10.5194/bg-15-937-2018

Rasilo, T., Y. T. Prairie, and P. A. del Giorgio. 2015. Large-scale patterns in summer diffusive CH_4 fluxes across boreal lakes, and contribution to diffusive C emissions. Glob. Change Biol. **21**: 1124–1139. doi:10.1111/gcb.12741

Riera, J. L., J. E. Schindler, and T. K. Kratz. 1999. Seasonal dynamics of carbon dioxide and methane in two clear-water lakes and two bog lakes in northern Wisconsin, U.S. A. Can. J. Fish. Aquat. Sci. **56**: 265–274. doi:10.1139/f98-182

Rosentreter, J. A., and others. 2021. Half of global methane emissions come from highly variable aquatic ecosystem sources. Nat. Geosci. **14**: 225–230. doi:10.1038/s41561-021-00715-2

Saarela, T., A. J. Rissanen, A. Ojala, J. Pumpanen, S. L. Aalto, M. Tiirola, T. Vesala, and H. Jäntti. 2019. CH_4 oxidation in a boreal lake during the development of hypolimnetic hypoxia. Aquat. Sci. **82**: 19. doi:10.1007/s00027-019-0690-8

Scandella, B. P., K. Delwiche, H. F. Hemond, and R. Juanes. 2017. Persistence of bubble outlets in soft, methane-generating sediments. J. Geophys. Res. Biogeo. **122**: 1298–1320. doi:10.1002/2016JG003717

Schwarz, J. I. K., W. Eckert, and R. Conrad. 2008. Response of the methanogenic microbial community of a profundal lake sediment (Lake Kinneret, Israel) to algal deposition. Limnol. Oceanogr. **53**: 113–121. doi:10.4319/lo.2008.53.1.0113

Segers, R. 1998. Methane production and methane consumption: A review of processes underlying wetland methane fluxes. Biogeochemistry **41**: 23–51. doi:10.1023/A:1005929032764

Sepulveda-Jauregui, A., K. M. Walter Anthony, K. Martinez-Cruz, S. Greene, and F. Thalasso. 2015. Methane and carbon dioxide emissions from 40 lakes along a north–south latitudinal transect in Alaska. Biogeosciences **12**: 3197–3223. doi:10.5194/bg-12-3197-2015

Steinman, A. D., G. A. Lamberti, and P. R. Leavitt. 2017. Biomass and pigments of benthic algae, p. 223–241. *In* Methods in stream ecology Academic Press

Thauer, R. K. 1998. Biochemistry of methanogenesis: A tribute to Marjory Stephenson. Microbiology **144**: 2377–2406.

Thilenius, J. F. 1995. Phytosociology and succession on earthquake-uplifted coastal wetlands, Copper River Delta, Alaska. PNW-GTR-346. PNW-GTR-346 U.S.D.A., Forest Service, Pacific Northwest Research Station.

Thottathil, S. D., P. C. J. Reis, and Y. T. Prairie. 2019. Methane oxidation kinetics in northern freshwater lakes. Biogeochemistry **143**: 105–116. doi:10.1007/s10533-019-00552-x

Tokida, T., T. Miyazaki, M. Mizoguchi, O. Nagata, F. Takakai, A. Kagemoto, and R. Hatano. 2007. Falling atmospheric pressure as a trigger for methane ebullition from peatland. Global Biogeochem. Cycles **21**: GB2003. doi:10.1029/2006GB002790

Vachon, D., T. Langenegger, D. Donis, and D. F. McGinnis. 2019. Influence of water column stratification and mixing patterns on the fate of methane produced in deep sediments of a small eutrophic lake. Limnol. Oceanogr. **64**: 2114–2128. doi:10.1002/lno.11172

Vizza, C., W. E. West, S. E. Jones, J. A. Hart, and G. A. Lamberti. 2017*a*. Regulators of coastal wetland methane production and responses to simulated global change. Biogeosciences **14**: 431–446. doi:10.5194/bg-14-431-2017

Vizza, C., J. A. Zwart, S. E. Jones, S. D. Tiegs, and G. A. Lamberti. 2017*b*. Landscape patterns shape wetland pond ecosystem function from glacial headwaters to ocean. Limnol. Oceanogr. **62**: S207–S221. doi:10.1002/lno.10575

Wagner, M., A. J. Roger, J. L. Flax, G. A. Brusseau, and D. A. Stahl. 1998. Phylogeny of dissimilatory sulfite reductases supports an early origin of sulfate respiration. J. Bacteriol. **180**: 2975–2982.

Walter Anthony, K. M., P. Anthony, G. Grosse, and J. Chanton. 2012. Geologic methane seeps along boundaries of Arctic permafrost thaw and melting glaciers. Nat. Geosci. **5**: 419–426. doi:10.1038/ngeo1480

Walter Anthony, K. M., D. A. Vas, L. Brosius, F. S. Chapin, S. A. Zimov, and Q. Zhuang. 2010. Estimating methane emissions from northern lakes using ice-bubble surveys. Limnol. Oceanogr.: Methods **8**: 592–609. doi:10.4319/lom.2010.8.0592

Walter, K. M., J. P. Chanton, F. S. Chapin, E. A. G. Schuur, and S. A. Zimov. 2008. Methane production and bubble emissions from arctic lakes: Isotopic implications for source pathways and ages. J. Geophys. Res. Biogeosci. **113**: G00A08. doi:10.1029/2007JG000569

West, W. E., J. J. Coloso, and S. E. Jones. 2012. Effects of algal and terrestrial carbon on methane production rates and methanogen community structure in a temperate lake sediment. Freshw. Biol. **57**: 949–955. doi:10.1111/j.1365-2427.2012.02755.x

West, W. E., K. P. Creamer, and S. E. Jones. 2016. Productivity and depth regulate lake contributions to atmospheric methane. Limnol. Oceanogr. **61**: S51–S61. doi:10.1002/lno.10247

West, W. E., S. M. McCarthy, and S. E. Jones. 2015. Phytoplankton lipid content influences freshwater lake methanogenesis. Freshw. Biol. **60**: 2261–2269. doi:10.1111/fwb.12652

Wetzel, R. G., and G. E. Likens. 2000. Composition and biomass of phytoplankton, p. 147–174. *In* Limnological analyses. Springer.

Whalen, S. C. 2005. Biogeochemistry of methane exchange between natural wetlands and the atmosphere. Environ. Eng. Sci. **22**: 73–94. doi:10.1089/ees.2005.22.73

Whiticar, M. J. 1999. Carbon and hydrogen isotope systematics of bacterial formation and oxidation of methane. Chem. Geol. **161**: 291–314. doi:10.1016/S0009-2541(99)00092-3

Wik, M., B. F. Thornton, D. Bastviken, J. Uhlbäck, and P. M. Crill. 2016*a*. Biased sampling of methane release from northern lakes: A problem for extrapolation. Geophys. Res. Lett. **43**: 1256–1262. doi:10.1002/2015GL066501

Wik, M., R. K. Varner, K. W. Anthony, S. MacIntyre, and D. Bastviken. 2016*b*. Climate-sensitive northern lakes and ponds are critical components of methane release. Nat. Geosci. **9**: 99–105. doi:10.1038/ngeo2578

Wilkinson, J., A. Maeck, Z. Alshboul, and A. Lorke. 2015. Continuous seasonal river ebullition measurements linked to sediment methane formation. Environ. Sci. Technol. **49**: 13121–13129. doi:10.1021/acs.est.5b01525

Zar, J. H. 2010. Biostatistical analysis, 5th ed. Pearson Prentice-Hall.

Zhao, K., E. W. Tedford, M. Zare, and G. A. Lawrence. 2021. Impact of atmospheric pressure variations on methane ebullition and lake turbidity during ice-cover. Limnol. Oceanogr. Lett. **6**: 253–261. doi:10.1002/lol2.10201

Zuur, A., E. N. Ieno, N. Walker, A. A. Saveliev, and G. M. Smith. 2009. Mixed effects models and extensions in ecology with R. Springer Science & Business Media.

Zverlov, V., M. Klein, S. Lücker, M. W. Friedrich, J. Kellermann, D. A. Stahl, A. Loy, and M. Wagner. 2005. Lateral gene transfer of dissimilatory (bi)sulfite reductase revisited. J. Bacteriol. **187**: 2203–2208. doi:10.1128/JB.187.6.2203-2208.2005

Acknowledgments

We thank the Cordova Ranger District of the USDA Forest Service for providing field and logistical support, particularly Deyna Kuntzsch, Andrew Morin, Sean Meade, Luca Adelfio, and Ken Hodges, without whom this work on the Copper River Delta would not have been possible. We also thank Gordie Reeves of the Pacific Northwest Research Station for his leadership and direction in the extensive research being conducted on the Copper River Delta. Mike Brueseke, Melanie Runkle, and Josephine Chau assisted with Chl *a* and SOM analyses. The Center for Environmental Science and Technology at UND provided instrumentation and analytical assistance for the chemical and stable isotope analyses. Funding was provided by the USDA Forest Service, the Pacific Northwest Research Station, the National Fish and Wildlife Foundation, the University of Notre Dame, and the National Science Foundation Graduate Research Fellowship Program. We also thank Jennifer Tank, the Kellogg Biological Station writing group, and the Roley Lab at WSU for their helpful feedback.

Conflict of Interest

None declared.

Submitted 06 March 2021
Revised 08 July 2021
Accepted 03 December 2021

Associate editor: John M. Melack